

liquid mercury (excess) for 30 min. Another  $\text{CH}_2\text{Cl}_2$  (10 mL) solution of  $\text{Et}_3\text{SiH}$  (5.0 mmol) was then added from the addition funnel. The rate of reaction, determined by following hydrogen evolution, was compared with the rate obtained in the absence of an inhibitor (Table II). In the Hg test, the rate of reaction was not affected by the presence of excess liquid mercury, and the surface of the mercury bead remained shiny at the end of the reaction. In the DCT test, a complete inhibition of catalysis was observed using 1 mol equiv of DCT.

**Observation of Intermediates Related to the Catalytic Cycle.** A typical experiment for the observation of **8** is described as follows.  $[\text{IrH}_2\text{S}_2(\text{PPh}_3)_2]\text{SbF}_6$  ( $\text{S} = \text{THF}$ ; **1a**; 40 mg, 0.036 mmol) was dissolved in rigorously dry  $\text{CD}_2\text{Cl}_2$  (0.5 mL) in an NMR tube. The sample was cooled to  $-80^\circ\text{C}$  (dry ice/acetone).  $\text{Et}_3\text{SiH}$  (10.8  $\mu\text{L}$ , 0.072 mmol) was added via a microsyringe under Ar. The sample was shaken and then

introduced into an NMR probe precooled to  $-80^\circ\text{C}$ . The solution gave the variable-temperature  $^1\text{H}$  NMR spectra as described in the text.

**$T_1$  Experiments.** The variable-temperature  $T_1$  measurements for the hydride resonances of **8** were carried out at 250 MHz in  $\text{CD}_2\text{Cl}_2$  at 193–273 K by the method of ref 37. The data obtained are reported as the following: temperature (K),  $T_1$  (ms, of the  $\text{IrH}$  resonance),  $T_1$  (ms, of the  $\text{Ir}(\eta^2\text{-HSiEt}_3)$ ). Only one average  $T_1$  can be measured above the coalescence temperature: 193, 653, 519; 203, 352, 315; 213, 267, 251; 223, 215, 212; 253, 212; 263, 326; 273, 454.

**Acknowledgment.** We thank the National Science Foundation for funding, X.-L.L. thanks the State Education Commission of the People's Republic of China for a fellowship, and we thank Prof. Dennis Lichtenberger for a preprint of his work.

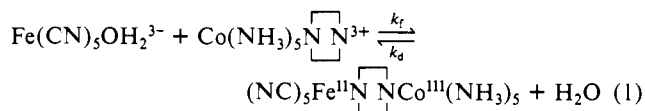
## Intramolecular Electron Transfer from Pentacyanoferrate(II) to Pentaamminecobalt(III) with 3,3'-Dimethyl-4,4'-bipyridine, 4,4'-Bipyridylacetylene, 1,4-Bis(4-pyridyl)butadiyne, 2,7-Diazapyrene, and 3,8-Phenanthroline as Bridging Ligands: Adiabaticity and the Role of Distance

Gyu-Hwan Lee, Leopoldo Della Ciana, and Albert Haim\*

Contribution from the Department of Chemistry, State University of New York, Stony Brook, New York 11794-3400. Received August 1, 1988

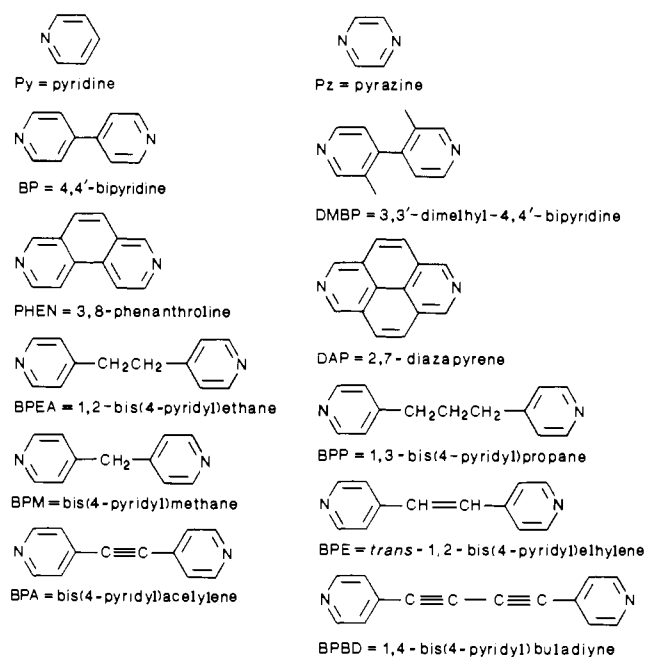
**Abstract:** Rate constants for intramolecular electron transfer from iron to cobalt in  $(\text{NH}_3)_5\text{Co}^{\text{III}}\text{LFe}^{\text{II}}(\text{CN})_5$  ( $\text{L} = 3,3'$ -dimethyl-4,4'-bipyridine, 4,4'-bipyridylacetylene, 1,4-bis(4-pyridyl)butadiyne, 2,7-diazapyrene, and 3,8-phenanthroline) have been measured at  $25^\circ\text{C}$  and ionic strength 0.10 M. The values of the rate constants (in the same order as the ligands above) are  $2.3 \times 10^{-3}$ ,  $1.7 \times 10^{-3}$ ,  $0.69 \times 10^{-3}$ ,  $4.2 \times 10^{-3}$ , and  $9.3 \times 10^{-3} \text{ s}^{-1}$ . The activation free energies for electron transfer display an inverse dependence with respect to the Fe–Co distance in the binuclear complexes. When these free energies are corrected for the solvent reorganization energies, the resulting corrected values are independent of distance and cover the narrow range  $13.5 \pm 0.5 \text{ kcal/mol}$ . The metal to ligand charge-transfer bands of  $\text{Fe}^{\text{II}}(\text{CN})_5\text{L}^{3-}$  complexes are shifted to higher energies when the remote N of L is coordinated to  $\text{Co}(\text{NH}_3)_5^{3+}$ . The shifts in energy are (in the same order as the ligands above) 4.0, 4.3, 1.7, 8.9, and 6.9 kcal/mol. On the basis of the observed trends, it is concluded that the intramolecular electron-transfer reactions proceed in the limiting adiabatic regime.

The measurement of intramolecular rather than intermolecular electron-transfer rates offers distinct advantages for investigating the details of the mechanism of electron transfer.<sup>1</sup> Complications involved in assembling the reactants are absent, and the transition state has a relatively well-defined geometry. Unfortunately, the search for systems feasible for intramolecular electron-transfer studies is beset by many difficulties.<sup>1</sup> It is not surprising, therefore, that there is only one type of system for which a wide range of precursor complexes that undergo intramolecular electron transfer can be prepared in high concentration by simply mixing two redox reagents.<sup>2</sup> In this type of system the lability of water in  $\text{Fe}(\text{CN})_5\text{OH}_2^{3-}$  and the affinity of the  $\text{Fe}(\text{CN})_5^{3-}$  moiety for aromatic nitrogen heterocycles ( $\text{N} \cdots \text{N}$ )<sup>3,4</sup> are exploited to generate precursor complexes  $(\text{NC})_5\text{Fe}^{\text{II}}\text{N} \cdots \text{NCo}^{\text{III}}(\text{NH}_3)_5$  in near quantitative yields from reaction 1. Once formed ( $k_f$  pathway), the precursor



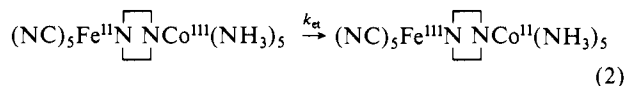
complexes generally disappear via intramolecular electron transfer

Chart 1



from Fe(II) to Co(III), eq 2 ( $k_{et}$  pathway), as well as dissociation into the reactants ( $k_d$  pathway).<sup>2</sup>

- (1) Haim, A. *Prog. Inorg. Chem.* **1983**, *30*, 273.
- (2) Haim, A. *Pure Appl. Chem.* **1983**, *55*, 89.
- (3) Toma, H. E.; Malin, J. M. *Inorg. Chem.* **1973**, *12*, 1039.
- (4) Toma, H. E.; Malin, J. M. *Inorg. Chem.* **1973**, *12*, 2080.



In this work, the coupling between donor ( $\text{Fe}^{\text{II}}$ ) and acceptor ( $\text{Co}^{\text{III}}$ ) sites via a series of aromatic nitrogen heterocycles was systematically investigated. Among the issues addressed, particular attention was given to the factors influencing the occurrence and degree of nonadiabaticity<sup>5</sup> and to the role of distance<sup>6</sup> in determining intramolecular electron-transfer rates. The ligands utilized in the present work are 3,3'-dimethyl-4,4'-bipyridine (DMBP), 4,4'-bipyridylacetylene (BPA), 1,4-bis(4-pyridyl)butadiyne (BPBD), 2,7-diazapyrene (DAP), and 3,8-phenanthroline (PHEN). The structures of these and other bridging ligands of interest are depicted in Chart I.

### Experimental Section

**Materials.** BPA was prepared as described in the literature.<sup>7</sup> *Caution!* The compound was found to cause blistering of the skin several days after contact. Protective gloves must be used in all manipulations involving this compound. DMBP was prepared according to a classical procedure.<sup>8</sup> The previously devised synthesis<sup>9</sup> was utilized to prepare BPBD. DAP and PHEN were prepared following established procedures.<sup>10-14</sup> *N*-methylpyrazinium perchlorate ( $\text{PzCH}_3^+\text{ClO}_4^-$ ) was prepared by methathesis of  $\text{PzCH}_3^+\text{I}^-$ <sup>15</sup> with sodium perchlorate.<sup>6</sup>

The water used in all experiments was house-distilled water passed through a Barnstead ion-exchange demineralizer and distilled in a modified, all-glass Corning Model AG-1b apparatus. The argon used to maintain anaerobic conditions was purified by passing it through a column of BTS catalyst kept at 110 °C. Lithium perchlorate (G. F. Smith) and sodium *p*-toluenesulfonate (NaPTS, Eastman Kodak) were recrystallized from redistilled water. All other reagents were used as received.

**Preparation of Complexes.** (Dimethyl sulfoxide)pentaamminecobalt(III) perchlorate dihydrate was synthesized by the literature procedure.<sup>16</sup> Sodium aminopentacyanoferrate(II) trihydrate<sup>17</sup> was purified as described previously.<sup>18</sup> Solutions of pentacyanoaquoferrate(II) [ $(1-2) \times 10^{-5}$  M] were prepared by aqution of  $\text{Na}_3[\text{Fe}(\text{CN})_5\text{NH}_3] \cdot 3\text{H}_2\text{O}$  in deaerated, pH 8.0, 0.010 M Tris buffer.

The following five pentaamminecobalt(III) complexes with some of the nitrogen heterocycles listed in Chart 1 were prepared by a procedure employed previously<sup>19</sup> to synthesize related complexes. (Dimethyl sulfoxide)pentaamminecobalt(III) perchlorate dihydrate (0.5 g for BPA, DMBP, BPBD; 0.2 g for DAP, PHEN) and the desired ligand (1 g for BPA, DMBP; 0.5 g for BPBD; 0.2 g for DAP, PHEN) were added to dimethyl sulfoxide (1 mL for BPA, DMBP; 3 mL for BPBD; 2 mL for DAP, PHEN) and heated to 90–95 °C (20 min for BPA, DMBP; 12 min for BPBD; 3 h for DAP; 30 min for PHEN). The resulting red-orange solutions were cooled to 0 °C and filtered if necessary (BPBD, DAP, PHEN; unreacted ligand is recovered in this step). A total of 20–30 mL of 0.10 M HCl was added, and the resulting solution was loaded on an ion-exchange column (Dowex 50W-X2, 200–400 mesh,  $\text{H}^+$  form for all complexes except BPBD; for the latter, Sephadex-SP-C25-120). The unreacted cobalt complex was eluted (2.0 M HCl for Dowex columns; 0.20 M HCl for Sephadex columns). Then, the desired product was eluted (4.0 M HCl for Dowex columns; 0.50 M HCl for Sephadex columns). In the case of DAP, the column was heated to ~50 °C with a flexible band heater because the complex salt crystallized inside the column. The yellow product solution was evaporated to dryness at ~45 °C in a rotary evaporator. The resulting solid was dissolved in the minimum amount of water, and then 72% perchloric acid was added dropwise until orange crystals formed. The mixture was kept at 0 °C for several hours and then filtered. The resulting solid was recrystallized

(5) Zawacky, S. K. S.; Taube, H. *J. Am. Chem. Soc.* **1981**, *103*, 3379.

(6) Szeeszy, A. P.; Haim, A. *J. Am. Chem. Soc.* **1981**, *103*, 1679.

(7) Tanner, M.; Ludi, A. *Chimia* **1980**, *34*, 23.

(8) Stoehr, C.; Wagner, M. *J. Prakt. Chem.* **1893**, *48*, 1.

(9) Dellaciana, L.; Haim, A. *J. Heterocycl. Chem.* **1984**, *21*, 607.

(10) Hunig, S.; Gross, J.; Lier, E. F.; Quast, H. *Justus Liebigs Ann. Chem.* **1973**, *339*.

(11) Lier, E. F.; Hunig, S.; Quast, H. *Angew. Chem.* **1978**, *80*, 799.

(12) Ruggli, P.; Schetty, O. *Helv. Chim. Acta* **1940**, *23*, 725.

(13) Gill, E. W.; Bracher, A. W. *J. Heterocycl. Chem.* **1983**, *20*, 1107.

(14) Schwann, T. J.; Miles, N. J. *J. Heterocycl. Chem.* **1982**, *19*, 1351.

(15) Bahner, C. T.; Norton, L. L. *J. Am. Chem. Soc.* **1950**, *72*, 2881.

(16) Piriz MacColl, C. R.; Beyer, L. *Inorg. Chem.* **1973**, *12*, 7.

(17) Brauer, G. *Handbook of Preparative Inorganic Chemistry*, 2nd ed.; Academic Press: New York, 1965; Vol. 2, p 1511.

(18) Jwo, J. J.; Haim, A. *J. Am. Chem. Soc.* **1976**, *98*, 1172.

(19) Jwo, J. J.; Gaus, P. L.; Haim, A. *J. Am. Chem. Soc.* **1979**, *101*, 6189.

**Table I.** MLCT Bands of Mononuclear and Binuclear Complexes of Pentacyanoferrate(II) with Nitrogen Heterocycles<sup>a</sup>

	$\lambda, ^b \text{ nm } (10^3 \times A, \text{ M}^{-1} \text{ cm}^{-1})^c$	
	$\text{Fe}(\text{CN})_5\text{L}^{3-}$	$(\text{NC})_5\text{Fe}^{\text{II}}\text{LCo}^{\text{III}}(\text{NH}_3)_5$
BPA	460 (7.6)	495 (7.6)
DMBP	383 (4.9)	405 (4.1)
BPBD	483 (9.0)	498 (6.7)
DAP	441 (5.3)	510 (4.0)
PHEN	456 (6.0)	512 (4.2)

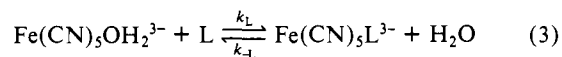
<sup>a</sup> Measured in aqueous solutions with  $[\text{Fe}(\text{CN})_5\text{L}^{3-}] = (1-2) \times 10^{-5}$  M,  $[\text{L}] \geq 2 \times 10^{-4}$  M,  $[\text{Co}(\text{NH}_3)_5\text{L}^{3+}] \sim 1 \times 10^{-3}$  M, ionic strength 0.10 M, pH 8. <sup>b</sup> Wavelength for maximum absorbance. <sup>c</sup> Molar absorbance at maximum.

2–3 times from aqueous perchloric acid; yields 40%, 50%, 15%, 30%, and 20% for the complexes with BPA, DMBP, BPBD, DAP, and PHEN, respectively. Anal. Calcd for  $[\text{Co}(\text{NH}_3)_5\text{NC}_5\text{H}_4\text{CC}_5\text{H}_4\text{NH}] \cdot (\text{ClO}_4)_4 \cdot 2\text{H}_2\text{O}$ : C, 18.99; H, 3.72; N, 12.92. Found: C, 18.87; H, 3.67; N, 12.86. Anal. Calcd for  $[\text{Co}(\text{NH}_3)_5\text{NC}_6\text{H}_6\text{C}_6\text{H}_6\text{NH}] \cdot (\text{ClO}_4)_4 \cdot 2\text{H}_2\text{O}$ : C, 18.89; H, 4.23; N, 12.85. Found: C, 18.97; H, 4.15; N, 12.75. Anal. Calcd for  $[\text{Co}(\text{NH}_3)_5\text{NC}_5\text{H}_4\text{CCCC}_5\text{H}_4\text{NH}] \cdot (\text{ClO}_4)_4 \cdot 2\text{H}_2\text{O}$ : C, 21.47; H, 3.60; N, 12.52. Found: C, 21.64; H, 3.57; N, 12.48. Anal. Calcd for  $[\text{Co}(\text{NH}_3)_5\text{NC}_5\text{H}_3\text{CHCHC}_5\text{H}_3\text{NH}] \cdot (\text{ClO}_4)_4 \cdot 2\text{H}_2\text{O}$ : C, 19.45; H, 3.54; N, 13.22. Found: C, 19.46; H, 3.79; N, 13.13. Anal. Calcd for  $[\text{Co}(\text{NH}_3)_5\text{NC}_5\text{H}_2\text{C}_4\text{H}_4\text{C}_5\text{H}_2\text{NH}] \cdot (\text{ClO}_4)_4 \cdot 2\text{H}_2\text{O}$ : C, 21.98; H, 3.42; N, 12.81. Found: C, 22.02; H, 3.37; N, 12.99.

**Physical Measurements.** Absorption spectra were measured in a Cary 118 spectrophotometer. Kinetic measurements of slow and fast reactions were carried out on a Cary 118 or a Durrum D-110 instrument, respectively. Data handling and processing was described previously in detail.<sup>20,21</sup> In all instances, first-order or pseudo-first-order conditions obtained and rate constants were calculated by nonlinear least-squares fitting of  $A_t$  to  $t$  according to  $A_t - A_\infty = (A_0 - A_\infty) \exp(-k_{\text{obs}}t)$ . pH and cyclic voltammetric measurements were carried out as described earlier.<sup>22</sup>

### Results

**Absorption Spectra.** Solutions of  $\text{Fe}(\text{CN})_5\text{L}^{3-}$  complexes were prepared via reaction 3. For L = DMBP and BPA, the solubilities of the ligands in water are sufficiently high that reaction 3 can be driven to substantial completion. In contrast, the solubilities



of DAP, PHEN, and BPBD in water are so low that it is not possible to drive reaction 3 to completion. Therefore, the following procedure was adopted. The ligands were dissolved in 40% methanol–water, and  $\text{Na}_3[\text{Fe}(\text{CN})_5\text{NH}_3] \cdot 3\text{H}_2\text{O}$  was added to the solution. After aqution of  $\text{Fe}(\text{CN})_5\text{NH}_3^{3-}$  to  $\text{Fe}(\text{CN})_5\text{OH}_2^{3-}$  and its subsequent reaction with the ligand, the solution was diluted with water (and filtered in the case of BPBD) and the absorption spectrum of the resulting solution (now containing <3% methanol) was recorded. Complexes of  $\text{Fe}(\text{CN})_5^{3-}$  with nitrogen heterocyclic ligands are characterized by a metal to ligand charge-transfer band (MLCT) in the visible or near-ultraviolet region.<sup>3</sup> The MLCT bands of the new complexes characterized in the present work are listed in Table I. The electronic spectra of the binuclear complexes are also characterized by similar, but transient, MLCT bands. Solutions of the complexes at ~10 °C were prepared via reaction 1. The absorption spectra of the solutions were obtained by repetitive scanning and extrapolation to the time of mixing. The MLCT bands of the binuclear complexes are also listed in Table I.

**Rates of Formation and Dissociation of  $\text{Fe}(\text{CN})_5\text{L}^{3-}$ .** Rates of formation of  $\text{Fe}(\text{CN})_5\text{L}^{3-}$  were obtained by mixing solutions of  $\text{Fe}(\text{CN})_5\text{OH}_2^{3-}$  with solutions of the desired ligand in the stopped-flow apparatus. The concentration of  $\text{Fe}(\text{II})$  was kept below  $2 \times 10^{-5}$  M to prevent its polymerization. Rates of dissociation of  $\text{Fe}(\text{CN})_5\text{L}^{3-}$  were obtained by employing ligand-exchange reactions.<sup>4</sup> Solutions of  $\text{Fe}(\text{CN})_5\text{L}^{3-}$  were prepared in situ by reaction of  $(1-2) \times 10^{-5}$  M  $\text{Fe}(\text{CN})_5\text{OH}_2^{3-}$  with the appropriate

(20) Akhtar, M. J.; Haim, A. *Inorg. Chem.* **1988**, *27*, 1608.

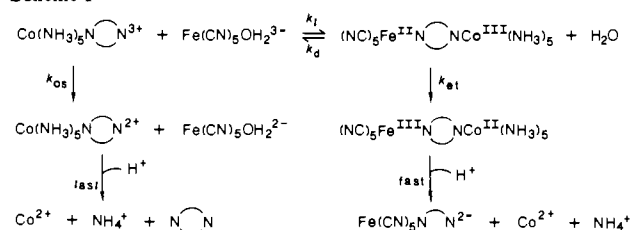
(21) Burewicz, A.; Haim, A. *Inorg. Chem.* **1988**, *27*, 1611.

(22) Yeh, A.; Haim, A. *J. Am. Chem. Soc.* **1985**, *106*, 369.

**Table II.** Rate Constants for Formation and Dissociation of Pentacyanoferrate(II) Complexes with Nitrogen Heterocycles<sup>a</sup>

L	$10^{-2} \times k_L, \text{M}^{-1} \text{s}^{-1}$	$10^4 \times k_{-L}, \text{s}^{-1}$	$10^{-5} \times k_L/k_{-L}$
BPA <sup>b</sup>	$5.7 \pm 0.5$	$7.5 \pm 0.4$	$7.6 \pm 0.7$
DMBP <sup>c</sup>	$4.8 \pm 0.3$	$7.3 \pm 0.1$	$6.6 \pm 0.3$
BPBD <sup>d</sup>	<i>e</i>	$6.2 \pm 0.1$	
DAP <sup>f</sup>	$1.8 \pm 0.1$	$6.6 \pm 0.2$	$2.7 \pm 0.2$
PHEN <sup>g</sup>	$2.7 \pm 0.1$	$6.5 \pm 0.1$	$4.1 \pm 0.4$
BP <sup>h</sup>	$3.0 \pm 0.1$	$8.0 \pm 0.1$	$3.8 \pm 0.2$

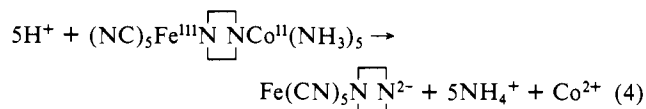
<sup>a</sup> At 25 °C, pH 8.0 (Tris buffer), ionic strength 0.10 M ( $\text{LiClO}_4$  for BPA, DMBP, and BPBD; NaPTS for DAP, PHEN, and BP),  $[\text{L}] = (0.5\text{--}2.0) \times 10^{-3} \text{ M}$ ,  $[\text{Fe}^{\text{II}}] = (1.0\text{--}2.0) \times 10^{-5} \text{ M}$ . <sup>b</sup> In the presence of 0.10 M pyridine; measurements at 460 nm. <sup>c</sup> In the presence of 0.070 M acetylpyridine; measurements of  $k_L$  at 383 nm; measurements of  $k_{-L}$  at 500 nm. <sup>d</sup> In the presence of 0.10 M pyridine; measurements at 483 nm. <sup>e</sup> BPBD is very insoluble and measurements of  $k_L$  are precluded. <sup>f</sup> In the presence of 0.10 M dimethylsulfoxide; measurements at 441 nm. <sup>g</sup> In the presence of 0.10 M dimethylsulfoxide; measurements at 456 nm. <sup>h</sup> In the presence of 0.10 M dimethyl sulfoxide; measurements at 432 nm.

**Scheme I**

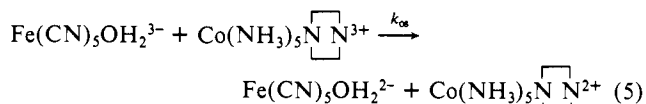
ligand ( $2 \times 10^{-4}\text{--}1 \times 10^{-3} \text{ M}$ ). Then, a large excess of ( $\sim 0.1 \text{ M}$ ) of the scavenging ligand (pyridine, dimethyl sulfoxide, acetylpyridine) was added. The formation and dissociation reactions were monitored spectrophotometrically at the wavelength of the MLCT band of  $\text{Fe}(\text{CN})_5\text{L}^{3-}$ . The rate constants  $k_L$  (eq 3) were calculated from  $k_{\text{obsd}}/[\text{L}]$  and are listed in column 2 of Table II. Rate constants for dissociation  $k_{-L}$  were taken to be equal to  $k_{\text{obsd}}$ . Equilibrium constants for reaction 3 were calculated as  $k_L/k_{-L}$  and are listed in column 4 of Table II. Measurements for 4,4'-bipyridine (BP) are included in Table II. These measurements in 0.10 M NaPTS are to be compared with earlier<sup>23</sup> measurements in 0.10 M  $\text{LiClO}_4$  ( $k_L = 4.0 \times 10^2 \text{ M}^{-1} \text{ s}^{-1}$ ,  $k_{-L} = 7.6 \times 10^{-4} \text{ s}^{-1}$ ).

**Rates of Formation, Dissociation, and Electron Transfer of Binuclear Complexes.** When a solution of  $\text{Fe}(\text{CN})_5\text{OH}_2^{3-}$  is mixed with a solution of a  $\text{Co}(\text{NH}_3)_5\text{N} \text{---} \text{N}^{3+}$  complex, high concentrations

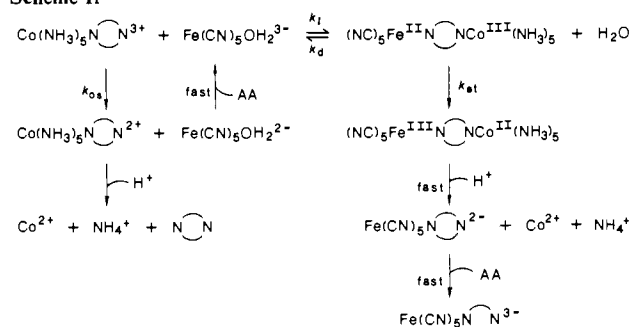
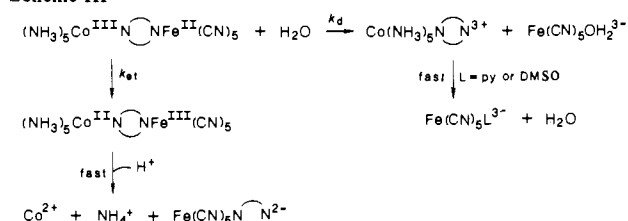
of  $(\text{NC})_5\text{Fe}^{\text{II}}\text{N} \text{---} \text{NCo}(\text{NH}_3)_5$  binuclear complexes are formed via reaction 1. Once formed, these binuclear complexes disappear by two parallel pathways. In the first, intramolecular electron transfer takes place (eq 2) and is followed by rapid ligand loss from Co(II), eq 4. The last reaction renders the intramolecular



electron-transfer step irreversible. Alternatively, the binuclear complexes can regenerate the starting reactants. The reactants can reform the binuclear complexes (eq 1) or undergo an outer-sphere redox reaction, eq 5. As in the intramolecular redox



process, the Co(II) produced loses its ligands rapidly. The complete set of reactions is summarized in Scheme I. It is clear that,

**Scheme II****Scheme III**

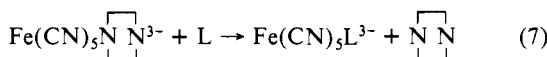
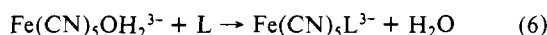
in order to obtain individual values of  $k_f$ ,  $k_d$ ,  $k_{el}$ , and  $k_{os}$ , at least four independent measurements need to be carried out. Two of the measurements relate to the formation and disappearance of the binuclear intermediates. It is noteworthy that the two processes occur in widely different time scales, namely, a few seconds and several minutes, respectively. Therefore, by monitoring the time-dependent increase in absorbance at the maximum for the MLCT band of the binuclear complex (in the stopped-flow apparatus) and the subsequent absorbance decrease (in the recording spectrophotometer), kinetic information regarding the formation and disappearance of the binuclear complexes is obtained. Quantitatively, according to Scheme I, the values of  $k_{\text{obsd}}$  calculated from the first-order absorbance increases and, denoted as  $k_A$ , are given by  $k_A = (k_f + k_{os})[\text{Co}(\text{NH}_3)_5\text{N} \text{---} \text{N}^{3+}]$ . The values of  $k_{\text{obsd}}$  calculated from the first-order absorbance decreases and, denoted as  $k_B$ , are given by  $k_B = k_{el} + k_d k_{os}/(k_f + k_{os})$ . When the formation and disappearance studies of the binuclear intermediates are carried out in the presence of added ascorbic acid,<sup>19</sup> Scheme II is applicable. Under these circumstances, the values of  $k_{\text{obsd}}$  obtained from the exponential absorbance increases and, denoted as  $k_C$ , are equal to  $k_f[\text{Co}(\text{NH}_3)_5\text{N} \text{---} \text{N}^{3+}]$ . In Scheme II the  $\text{Fe}(\text{CN})_5\text{OH}_2^{3-}$  produced in the outer-sphere pathway is rapidly reduced to  $\text{Fe}(\text{CN})_5\text{OH}_2^{3-}$ , and therefore the  $k_{os}$  path does not contribute to the net disappearance of  $\text{Fe}(\text{CN})_5\text{OH}_2^{3-}$ . According to Scheme II, the absorbance decrease is governed only by  $k_{el}$ . However, under these conditions, the reaction becomes catalytic rather than stoichiometric. The  $\text{Fe}^{\text{III}}(\text{CN})_5\text{N} \text{---} \text{N}^{2-}$  produced in the intramolecular electron-transfer pathway is rapidly reduced by ascorbic acid to  $\text{Fe}^{\text{II}}(\text{CN})_5\text{N} \text{---} \text{N}^{3-}$ , which in turn loses the ligand  $\text{N} \text{---} \text{N}$  and produces  $\text{Fe}(\text{CN})_5\text{OH}_2^{3-}$ . The latter reacts with the excess  $\text{Co}(\text{NH}_3)_5\text{N} \text{---} \text{N}^{3+}$  complex and produces more binuclear complex, which in turn undergoes internal transfer to produce  $\text{Fe}(\text{CN})_5\text{N} \text{---} \text{N}^{2-}$ . Therefore, measurements of the absorbance decreases in the presence of ascorbic acid were discontinued after the catalytic process was discovered. In a third type of experiment,<sup>19</sup> the iron and cobalt reactants were mixed, the binuclear complexes were allowed to form and, when they had reached their maximum concentration, an excess of a scavenging ligand (pyridine or dimethyl sulfoxide) was added. Under these circumstances, Scheme III, the binuclear complexes disappear via two parallel first-order pathways. The rate constant measured from the ex-

**Table VII.** Kinetic Analysis for Reactions Pertaining to Binuclear Complexes  $(\text{NH}_3)_5\text{CoLFe}(\text{CN})_5^a$ 

L	$10^{-3} \times k_f$ , $\text{M}^{-1} \text{s}^{-1}$	$10^3 \times k_d$ , $\text{s}^{-1}$	$10^3 \times k_{et}$ , $\text{s}^{-1}$	$10^{-2} \times k_{os}$ , $\text{M}^{-1} \text{s}^{-1}$
BP <sup>b</sup>	$5.5 \pm 0.3$	$3.9 \pm 0.3$	$2.0 \pm 0.1$	$5.7 \pm 0.5$
BP <sup>c</sup>	$2.9 \pm 0.2$	$3.1 \pm 0.2$	$2.6 \pm 0.2$	$1.4 \pm 0.2$
DMBP	$1.2 \pm 0.1$	$2.5 \pm 0.1$	$2.3 \pm 0.1$	$1.9 \pm 0.2$
BPA	$2.9 \pm 0.1$	$1.0 \pm 0.1$	$1.7 \pm 0.1$	$3.8 \pm 0.4$
BPE	$2.1 \pm 0.1$	$2.9 \pm 0.1$	$1.4 \pm 0.2$	$1.2 \pm 0.5$
BPBD	$0.50 \pm 0.02$	$2.2 \pm 0.1$	$0.69 \pm 0.04$	$2.9 \pm 0.3$
PHEN	$1.8 \pm 0.1$	$2.8 \pm 0.2$	$4.2 \pm 0.2$	$1.1 \pm 0.2$
DAP	$1.6 \pm 0.1$	$3.9 \pm 0.2$	$9.3 \pm 0.1$	$1.5 \pm 0.3$

<sup>a</sup> At 25 °C, pH 8 (Tris buffer), ionic strength 0.10 M. <sup>b</sup> LiClO<sub>4</sub>. <sup>c</sup> NaPTS.

ponential absorption decrease and, denoted as  $k_E$ , is simply  $k_d + k_{et}$ . Stoichiometric measurements were carried out to determine the concentrations of  $\text{Fe}(\text{CN})_5\text{N}^{\text{N}2-}$  produced in experiments where the disappearance of the binuclear complexes was followed in the absence of ascorbic acid or scavenging ligand (experiments where  $k_b$  was obtained). The product solutions were treated with an excess of ligand (pyridine, 4-acetylpyridine, or *N*-methylpyrazinium) and then with ascorbic acid. The two reaction products  $\text{Fe}(\text{CN})_5\text{N}^{\text{N}2-}$  and  $\text{Fe}(\text{CN})_5\text{OH}_2^{2-}$  are reduced rapidly by ascorbic acid, and then  $\text{Fe}(\text{CN})_5\text{L}^{3-}$  (L = pyridine, 4-acetylpyridine, or *N*-methylpyrazinium) is formed by two substitution processes, one rapid, eq 6, and one slow, eq 7. Ac-

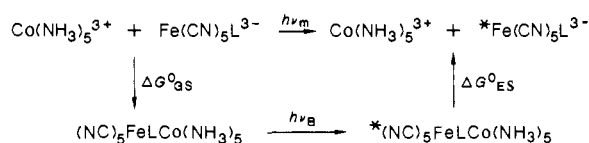


ordingly, the rapid and slow absorbance changes that are observed at the absorption maximum of  $\text{Fe}(\text{CN})_5\text{L}^{3-}$  upon addition of L and ascorbic acid to the product solution are a measure of the  $\text{Fe}(\text{CN})_5\text{OH}_2^{2-}$  and  $\text{Fe}(\text{CN})_5\text{N}^{\text{N}2-}$  produced. The ratio *R* of  $[\text{Fe}(\text{CN})_5\text{OH}_2^{2-}]$  to  $[\text{Fe}(\text{CN})_5\text{N}^{\text{N}2-}]$  is given, according to Scheme I, by  $k_{os}(k_{e1} + k_d)/k_{e1}k_f$ . Values of the measured rate constants  $k_A$ ,  $k_B$ ,  $k_C$ , and  $k_E$  and of the stoichiometric ratios *R* are listed in Tables III–VI (supplementary material). The calculated values of  $k_d$ ,  $k_f$ ,  $k_{os}$ , and  $k_{e1}$  are listed in Table VII.

## Discussion

**Electronic Spectra.** Much of the chemistry of  $\text{Fe}^{\text{II}}(\text{CN})_5\text{L}$  complexes is dominated by  $\Pi$  back-bonding interaction between the filled  $t_{2g}$  ( $d_{\Pi}$ ) orbitals of the Fe(II) and the unoccupied  $\Pi^*$  orbitals of the aromatic nitrogen heterocycles. The electronic spectra of these species feature intense, low-energy metal to ligand charge-transfer (MLCT) bands.<sup>3</sup> Specifically, these MLCT transitions can be described as involving ground states largely metal centered,  $d_{\Pi}$  (M) in character, and excited states largely ligand centered,  $\Pi^*$  (L) in character. It has been shown<sup>3</sup> that the energies of the MLCT bands are very sensitive to substituent changes on L. Electron-withdrawing substituents cause a bathochromic shift in the MLCT maximum, whereas electron-releasing substituents produce a hypsochromic shift, the effects being particularly important in positions conjugated to the bound nitrogen. We suggested previously<sup>19</sup> that an analysis of these effects can provide clues concerning the extent of electronic communication between the Fe(II) and the Co(III) metal centers in  $(\text{NC})_5\text{FeLCo}(\text{NH}_3)_5$  binuclear complexes. In turn this information is of considerable value in shedding light on the intramolecular electron-transfer processes taking place in the binuclear complexes. It was noted previously<sup>19</sup> that coordination of the  $\text{Co}(\text{NH}_3)_5^{3+}$  moiety to the remote N in  $\text{Fe}(\text{CN})_5\text{L}^{3-}$  for L = Pz, BP, or BPE substantial bathochromic shifts in the MLCT bands, whereas no shifts occur for L = BPM or BPP. These results indicate that uninterrupted conjugation between the two pyridine rings is required for transmission of the electron-withdrawing effect

## Scheme IV



of  $\text{Co}(\text{NH}_3)_5^{3+}$ . These observations were rationalized by analysis of the mechanism by which the Fe(II) and Co(III) centers communicate. The ligands BP and BPE allow delocalization of negative charge from the Fe(II)  $t_{2g}$  orbitals into the remote pyridine ring through resonance forms such as



Clearly, the above resonance forms will be stabilized by attachment of the electron-withdrawing moiety  $\text{Co}(\text{NH}_3)_5^{3+}$  to the remote N and, as a consequence, the MLCT band will shift to lower energy. By contrast, for  $\text{Fe}(\text{CN})_5\text{L}^{3-}$  (L = BPM, BPP) where conjugation between the pyridine rings is interrupted, no obvious mechanism for delocalization of iron electrons is available. As a result, electron-withdrawing effects are not transmitted and coordination of the electropositive substituent  $\text{Co}(\text{NH}_3)_5^{3+}$  to the remote N results in no shift of the MLCT band.

Although all the ligands studied in the present work feature uninterrupted conjugation between the pyridine rings and are therefore capable of transmitting electron-withdrawing effects, the various ligands do so with different degrees of efficiency. The steric constraints associated with the methyl groups in the 3,3' positions in the ligand DMBP prevent the pyridine rings from adopting the coplanar conformation necessary for good coupling. Thus, when the H in the para position of the pyridine ring in  $\text{Fe}(\text{CN})_5\text{L}^{3-}$  (L = pyridine) is replaced by the electron-withdrawing group pyrid-4-yl, the energy of the MLCT band shifts by  $0.44 \mu\text{m}^{-1}$  to the red. In contrast, a much smaller bathochromic shift ( $0.15 \mu\text{m}^{-1}$ ) is observed in the MLCT maximum of  $\text{Fe}(\text{CN})_5\text{L}^{3-}$  when pyridine is replaced by DMBP. Even when the inductive effects of the methyl groups are considered, it is apparent that the transmission of electronic withdrawing effects of the remote pyridine is considerably less efficient for DMBP than for BP. Moreover, the coordination of  $\text{Co}(\text{NH}_3)_5^{3+}$  to the remote N of  $\text{Fe}(\text{CN})_5\text{DMBP}^{3-}$  results in a modest bathochromic shift ( $0.14 \mu\text{m}^{-1}$ ) whereas the shift is considerably larger for the BP system ( $0.34 \mu\text{m}^{-1}$ ). Additional evidence for diminished coupling between the two pyridine rings of BP when two methyl groups are placed in the 3,3' positions comes from calculations of the coupling parameters from the observed intervalence bands in the mixed-valence compounds  $(\text{NH}_3)_5\text{RuL}(\text{NH}_3)_5^{2+}$ .<sup>23</sup> The values of the interaction energy  $2H_{12}$  (the energy splitting in the intersection region) are 2.2 and 1.1 kcal/mol for BP and DMBP, respectively.<sup>23</sup>

The magnitude of the bathochromic shift in the MLCT energy of  $\text{Fe}(\text{CN})_5\text{L}^{3-}$  complexes, which occurs upon coordination of  $\text{Co}(\text{NH}_3)_5^{3+}$  to the remote N of the ligand L, decreases with increasing length of the ligand L. Thus, values of  $\Delta\nu$  (in  $\mu\text{m}^{-1}$ ) the difference between the frequencies of the maxima of the MLCT bands of the mononuclear and binuclear complexes and of the metal to metal distance (in Å) in the binuclear complexes are: Pz, 0.63 and 6.8; BP, 0.34 and 11.3; BPA, 0.15 and 13.5; BPBD, 0.06 and 16.1. Evidently, the increase in bridge length attenuates the communication between centers, a result consistent with rules<sup>24</sup> enunciated for  $\Pi$ -mediated interactions between donor and acceptor orbitals of  $\Pi$  symmetry, in the present case, the  $d_{\Pi}$  orbital of the iron center and the  $p_{\Pi}$  orbital of the remote N. An alternate (and instructive) way of examining the attenuation of remote group substituent effects with an increase in bridge length makes use of the quasi-thermodynamic cycle in Scheme IV.  $\nu_m$  and  $\nu_B$  are the frequencies of the MLCT bands of mononuclear and binuclear complexes, respectively.  $\Delta G_{GS}^{\circ}$  and  $\Delta G_{ES}^{\circ}$  are the

Table VIII. Rate Constants, Free Energy Barriers, and Free Energies for Solvent Reorganization in Intramolecular Electron-Transfer Reactions of Complexes  $(\text{NC})_5\text{Fe}^{\text{II}}\text{LCo}^{\text{III}}(\text{NH}_3)_5$

ligand <sup>a</sup>	$k_{\text{et}}$ , <sup>b</sup> s <sup>-1</sup>	$d$ , Å	$\Delta G^*$ , <sup>c</sup> kcal/mol	$\Delta G_{\text{os}}^*$ , <sup>d</sup> kcal/mol	$\Delta G_{\text{corr}}^*$ , <sup>e</sup> kcal/mol
Pz	$5.5 \times 10^{-2}$	6.8	19.4	4.7 (4.9)	14.7
BP	$2.7 \times 10^{-3}$	11.3	21.2	6.9 (7.5)	14.3
DMBP	$2.3 \times 10^{-3}$	11.3	21.3	6.9 (7.5)	14.4
DAP	$9.3 \times 10^{-3}$	11.3	20.4	6.9 (7.5)	13.5
PHEN	$4.2 \times 10^{-3}$	11.3	20.9	6.9 (7.5)	14.0
BPE	$1.4 \times 10^{-3}$	13.5	21.6	7.5 (8.2)	14.1
BPA	$1.7 \times 10^{-3}$	13.6	21.5	7.5 (8.2)	14.0
BPBD	$6.9 \times 10^{-4}$	16.1	22.0	8.1 (8.7)	13.9

<sup>a</sup> See Chart 1 for structures. <sup>b</sup> At 25 °C and 0.10 M ionic strength. <sup>c</sup> Calculated from eq 8. <sup>d</sup> Calculated from the ellipsoidal cavity model. Value in parentheses calculated from eq 10. <sup>e</sup>  $\Delta G^* - \Delta G_{\text{os}}^*$ .

standard free energy changes for formation of binuclear complexes in ground and excited states, respectively. The difference between  $h\nu_{\text{m}}$  and  $h\nu_{\text{B}}$  is a measure of the relative affinity for  $\text{Co}(\text{NH}_3)_5^{3+}$  of a remote N in a ground-state and in an excited-state  $\text{Fe}(\text{CN})_5\text{L}^{3-}$  complex. Values of  $h\nu_{\text{m}} - h\nu_{\text{B}}$  (in kcal) for Pz, BP, BPA, and BPBD are 18.0, 9.4, 4.3, and 1.7, respectively. Since  $\text{Co}(\text{NH}_3)_5^{3+}$  is a  $\sigma$  acid with no  $\Pi$ -donating or -accepting ability, the difference  $h\nu_{\text{m}} - h\nu_{\text{B}} = \Delta G_{\text{GS}}^\circ - \Delta G_{\text{ES}}^\circ$  is a measure of the increased  $\sigma$  basicity of the remote N in  $^*\text{Fe}(\text{CN})_5\text{L}^{3-}$  vs  $\text{Fe}(\text{CN})_5\text{L}^{3-}$  and presumably of the increased negative charge on the remote N. Evidently, as ascertained by the sharp decrease in  $\Delta G_{\text{GS}}^\circ - \Delta G_{\text{ES}}^\circ$  along the series Pz, BP, BPA, and BPBD, the shift in electron density from iron to ligand accompanying light absorption by  $\text{Fe}(\text{CN})_5\text{L}^{3-}$  results in an enormous increase in charge density at the remote N when L is Pz ( $\Delta G_{\text{GS}}^\circ - \Delta G_{\text{ES}}^\circ = 18.0$  kcal), whereas a modest increase occurs when L is BPBD ( $\Delta G_{\text{ES}}^\circ = 1.7$  kcal). Clearly, transfer of electron density from the iron center to the remote N in  $\text{Fe}(\text{CN})_5\text{L}^{3-}$  becomes less effective as the length of L increases.

**Intramolecular Electron Transfer.** Rate constants for intramolecular electron transfer for the complexes studied in the present work as well as for related complexes from previous studies<sup>19,25,26</sup> are listed in column 2 of Table VIII.

According to current views<sup>27</sup> in electron-transfer theory, rate constants for intramolecular electron transfer within a ligand-bridged binuclear complex (inner-sphere) or a reactant pair (outer-sphere) are given by eq 8 where  $\nu_n$  is an effective nuclear frequency (taken to be  $10^{13}$  s<sup>-1</sup>),  $\kappa_e$  is the electronic factor (equal

$$k_{\text{el}} = \nu_n \kappa_e e^{-\Delta G^*/RT} \quad (8)$$

to 1 for adiabatic reactions and less than 1 for nonadiabatic reactions), and  $\Delta G^*$  is the reorganization free energy. The latter is related to  $\Delta G_{\text{in}}^*$  and  $\Delta G_{\text{out}}^*$ , the inner- and outer-shell (solvent) reorganization energies, respectively, and to  $\Delta G_{\text{el}}^\circ$ , the standard free energy change for intramolecular electron transfer, by eq 9.<sup>27</sup>

$$\Delta G^* = \Delta G_{\text{in}}^* + \Delta G_{\text{out}}^* + \frac{\Delta G_{\text{el}}^\circ}{2} + \frac{(\Delta G_{\text{el}}^\circ)^2}{16(\Delta G_{\text{in}}^* + \Delta G_{\text{out}}^*)} \quad (9)$$

The expression for  $\Delta G_{\text{out}}^*$  on the basis of the two-sphere, continuum dielectric model is given in eq 10 where  $\Delta e$  is the charge

$$\Delta G_{\text{out}}^* = \frac{(\Delta e)^2}{4} \left( \frac{1}{2r_1} + \frac{1}{2r_2} - \frac{1}{d} \right) \left( \frac{1}{D_{\text{op}}} - \frac{1}{D_s} \right) \quad (10)$$

transferred in the reaction,  $D_{\text{op}}$  and  $D_s$  are the optical and static dielectric constants of the solvent, respectively,  $r_1$  and  $r_2$  are the radii of the reactants (assumed to be spherical), and  $d$  is the distance between the metal centers. In the harmonic oscillator approximation  $\Delta G_{\text{in}}^*$  is given by eq 11 where  $f_i$  is a reduced force

$$\Delta G_{\text{in}}^* = \frac{1}{2} \sum f_i (\Delta d_i^\circ)^2 \quad (11)$$

constant equal to  $2f_i^{\text{A}}f_i^{\text{B}}/(f_i^{\text{A}} + f_i^{\text{B}})$ ,  $\Delta d_i^\circ = |d_i^{\text{A}} - d_i^{\text{B}}|$  is the difference in the equilibrium metal-ligand distances in the two oxidation states, and the summation is carried out over all vibrations. According to eq 8-11, the rate constant for an intramolecular electron-transfer reaction depends on an electronic factor ( $\kappa_e$ ), a nuclear factor ( $\Delta G_{\text{in}}^* + \Delta G_{\text{out}}^*$ ), and a thermodynamic factor ( $\Delta G_{\text{el}}^\circ$ ). The role played by these factors in the reactions under consideration will be now examined in detail.

We noted previously<sup>6</sup> that the reorganization free energies for the reactions of the binuclear complexes under consideration are inversely proportional to the distance between the metal centers. With the addition of the BPBD complex, the metal centers separation covers the range from 6 to 16 Å. In order to rationalize this observation, it was assumed<sup>6</sup> that the first and last two terms in eq 9 remain pretty constant along the series of complexes. Under these circumstances, with  $\Delta G_{\text{out}}^*$  given by eq 10, it was shown<sup>6</sup> that  $\Delta G^* = \text{intercept} - \text{slope}/d$ , where slope = 45 kcal if  $d$  is expressed in angstroms. The experimental slopes for the  $(\text{NC})_5\text{FeLCo}(\text{NH}_3)_5$  and  $(\text{NH}_3)_4(\text{OH})_2\text{RuLCo}(\text{NH}_3)_5^{5+}$  systems were 30.9 and 33.4 kcal, respectively.<sup>6</sup> The reasonable agreement between experimental and theoretical slopes was taken to provide justification for the above assumptions, and we inferred that the distance dependence of the rate constants was determined by the solvent reorganization free energies. We now reexamine and confirm most of the above assumptions. It is likely that  $\Delta G_{\text{el}}^\circ$  does not change much along the series of substituted pyridine complexes in Table VIII, but there is a question for the pyrazine complex. Although  $\Delta G_{\text{el}}^\circ$  values cannot be measured (because of the irreversibility of the  $\text{Co}^{\text{III}}\text{-Co}^{\text{II}}$  couple), reasonable estimates of the reduction potentials at the iron site can be made for Pz and BP. The binuclear complexes  $(\text{NC})_5\text{Fe}^{\text{II}}\text{LRh}^{\text{III}}(\text{NH}_3)_5$  are good models for the corresponding  $\text{Co}^{\text{III}}$  complexes.<sup>22</sup> The values of  $E^\circ$  for the iron site are 0.71 and 0.52 V for Pz and BP, respectively. Unless, fortuitously, the  $E^\circ$  for the cobalt site varies by the same amount as the iron site, it is evident that the  $\Delta G_{\text{el}}^\circ$  values for Pz and BP are going to be different. On the other hand, there is some evidence, albeit indirect, that the  $E^\circ$  values for the iron site remain relatively constant along the series of pyridine complexes. We have measured<sup>28</sup> the reduction potentials of several binuclear complexes  $(\text{EDTA})\text{Ru}^{\text{III}}\text{LCo}^{\text{III}}(\text{NH}_3)_5^{2+}$ . Values of  $E^\circ$  for BP, DMBP, BPE, and BPBD are 0.13, 0.12, 0.11, and 0.15 V, respectively. Moreover, we have found<sup>28</sup> that plots of  $E^\circ$  for  $\text{Ru}(\text{EDTA})\text{L}^{2-}$  vs  $E^\circ$  for  $\text{Fe}(\text{CN})_5\text{L}^{2-}$  are linear and have a slope of  $\sim 1$ . On the basis of these findings, it is reasonable to postulate that  $E^\circ$  values for  $(\text{NC})_5\text{FeLCo}(\text{NH}_3)_5^{+0}$  couples (L = BP, DMBP, BPE, BPBD) are, as found<sup>28</sup> for the analogous  $\text{Ru}(\text{EDTA})$  couples, relatively insensitive to the identity of the pyridine ligand. Since the  $\text{Co}(\text{NH}_3)_5^{3+}$  moiety is neither a  $\Pi$  donor nor a  $\Pi$  acceptor, the  $E^\circ$  at the Co site of the binuclear complexes will not change<sup>29,30</sup> with peripheral changes in the pyridine ligand. Therefore, the driving forces for the reactions will remain constant. The second assumption made earlier<sup>6</sup> was that the first term in eq 9 does not change much as the bridging ligand length is changed. Since inner-shell reorganization energies are determined by the immediate coordination environment of the metal centers,<sup>27,29</sup> it seems clear that  $\Delta G_{\text{in}}^*$  will be nearly constant. Finally, it was assumed<sup>6</sup> that the last term in eq 9 is insensitive to donor-acceptor separation. Evidently, this assumption cannot be correct since  $\Delta G_{\text{out}}^*$  changes with the distance between metal centers. However, as will be seen presently, it is likely that the last term in eq 9 is small compared to the other terms. Although values of  $\Delta G_{\text{el}}^\circ$  are not known, an estimate can be made based on the  $E^\circ$  values for the Fe and the Co centers. The values for the Fe sites can be estimated fairly accurately from the values

(28) Oliveira, L. A. A.; Della Ciana, L.; Haim, A., to be submitted for publication.

(29) Taube, H. In *Tunneling in Biological Systems*, Chance, B., DeVault, D. C., Frauenfelder, H., Marcus, R. A., Schrieffer, J. B., Sutin, N., Eds.; Academic Press: New York, 1979; p 173.

(30) Schaffer, L. J.; Taube, H. *J. Phys. Chem.* **1986**, *90*, 3669.

(25) Gaswick, D.; Haim, A. *J. Am. Chem. Soc.* **1974**, *96*, 7845.

(26) Malin, J.; Ryan, D. A.; O'Halloran, T. V. *J. Am. Chem. Soc.* **1978**, *100*, 2097.

(27) Sutin, N. *Prog. Inorg. Chem.* **1983**, *30*, 441.

**Table IX.** Equilibrium Constants and Rate Constants for Formation and Dissociation of  $\text{Fe}(\text{CN})_5^{n-}$  Complexes<sup>a</sup>

L	$k_L \times 10^2$ , $\text{M}^{-1} \text{s}^{-1}$	$k_{-L} \times 10^{-7}$ , $\text{s}^{-1}$	$K_L \times 10^5$ , $\text{M}^{-1}$	$k_f \times 10^2$ , $\text{M}^{-1} \text{s}^{-1}$	$k_d \times 10^{-4}$ , $\text{s}^{-1}$	$K_L \times 10^5$ , $\text{s}^{-1}$
Pz	3.8	4.2	9.0	70	7.4	9.5
BP	4.1	7.8	5.2	55	39	14
BPA	5.7	7.5	7.6	29	10	29
BPBD		6.2		5.0	22	2.4

<sup>a</sup> At 25 °C. <sup>b</sup> Distance between Fe and Co in binuclear complex.

for the corresponding Fe–Rh binuclear complexes. These values are 0.71 and 0.54 V for Pz and BPY, respectively.<sup>22</sup> The  $E^\circ$  values for the Co site has been estimated at about 0.10 V.<sup>31</sup> On the basis of these estimates, the values of  $\Delta G_{\text{el}}^\circ$  for Pz and BPY are 14 and 10 kcal/mol, respectively. Values of  $\Delta G_{\text{in}}^*$  for the Co<sup>31</sup> and Fe<sup>32</sup> moieties have been estimated at 8.6 and 0.3 kcal/mol, respectively. Estimates of  $\Delta G_{\text{out}}^*$  will be presented below, the values being 4.7, 6.9, and 8.7 kcal/mol for Pz, BP, and BPBD, respectively. Therefore, the last term in eq 9 has values of 0.9, 0.4, and 0.3 kcal/mol for Pz, BP, and BPBD, respectively. Evidently, the contribution of the last term (0.3–0.9 kcal) to the total value of  $\Delta G^\circ$  (~19–22 kcal) is rather minor, as assumed earlier.<sup>6,33</sup> Therefore, any distance dependence of the observed rate constants is associated with the outer-sphere reorganization and/or the electronic factor.

We are now in a position to comment on the adiabaticity or nonadiabaticity (electronic factor) of the reactions under consideration. Since our initial<sup>6</sup> publication on the role of distance in intramolecular electron transfer, other authors<sup>31,34</sup> have reiterated the need to factor out the solvent reorganization contribution in order to examine the distance dependence of the electronic factor contribution to intramolecular electron transfer. Values of  $\Delta G_{\text{out}}^*$  calculated from the two-sphere model (eq 10) and from the more realistic minimum enclosed volume ellipsoidal cavity model<sup>35</sup> are listed in column 5 of Table VIII. Observed values of  $\Delta G^*$  and values of  $\Delta G_{\text{corr}}^* = \Delta G^* - \Delta G_{\text{out}}^*$  are plotted vs  $1/d$  in Figure 1. It will be seen that, as found earlier,<sup>6</sup>  $\Delta G^*$  varies linearly with  $1/d$  but, in contrast,  $\Delta G_{\text{corr}}^*$  is independent of  $d$ . In other words, once the effect of solvent polarization is factored out, the rate constants for intramolecular electron transfer are independent of donor–acceptor separation. On the basis of eq 8, this result implies that the electronic factor  $\kappa$  is constant for a series of bridging ligands of varying length. Since  $\kappa$  would be anticipated to decrease with increasing metal to metal distance,<sup>27,29,34,36</sup> we infer with confidence that the adiabatic limit has been reached for all these reactions; e.g.,  $\kappa = 1$ . This conclusion is reinforced by comparing the distance dependence of  $\Delta G_{\text{corr}}^*$  and of  $h\nu_M - h\nu_B$ . It will be seen (Figure 1) that, in contrast with  $\Delta G_{\text{corr}}^*$  which is independent of  $d$ ,  $h\nu_M - h\nu_B$  decreases precipitously with increasing Fe–Co distance. As noted earlier, the dramatic decrease in  $h\nu_M - h\nu_B$  with increasing metal centers separation indicates that a substantial reduction in the coupling between metal centers obtains as the length of the bridging ligand increases. Since the rate of electron transfer (corrected for solvent reorganization) is insensitive to the magnitude of the coupling, it is reasonable to infer that rate saturation with respect to the electronic factor has been attained and that all of the reactions proceed in the adiabatic regime. A particularly significant result involves the ligands BP, where the two pyridine rings are free to achieve coplanarity, and DMBP, where the steric factor associated with the 3-methyl groups causes the pyridine rings to be perpendicular to each other. The coupling between the pyridine rings is considerably smaller for DMBP than for BP. The MLCT bands

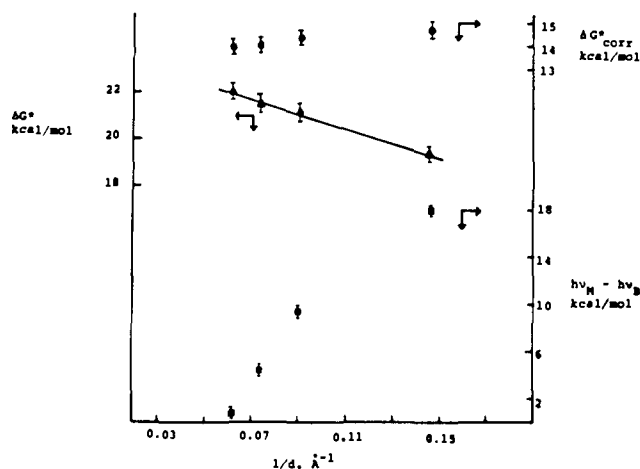


**Figure 1.**  $\Delta G^*$ ,  $\Delta G_{\text{corr}}^*$ , and  $h\nu_M - h\nu_B$  (in kcal/mol) vs  $1/d$  (in  $\text{\AA}^{-1}$ ). From left to right, the entries are for BPBD, BPA, BP, and Pz.

of  $\text{Fe}(\text{CN})_5\text{Py}^{3-}$ ,  $\text{Fe}(\text{CN})_5\text{BP}^{3-}$ , and  $\text{Fe}(\text{CN})_5\text{DMBP}^{3-}$  occur at 362, 432, and 383 nm, respectively. Even taking into account the inductive effects of the methyl groups, it is evident that the transmission of the electron-withdrawing effect of the remote pyridine group is much less efficient for the dimethyl derivative than for the unsubstituted ligand. Moreover, addition of  $\text{Co}(\text{NH}_3)_5^{3+}$  to the remote N of  $\text{Fe}(\text{CN})_5\text{BP}^{3-}$  results in a large bathochromic shift (432–505 nm, 9.4 kcal) whereas the shift is less than half (383–405 nm, 4.0 kcal) for coordination of  $\text{Co}(\text{NH}_3)_5^{3+}$  to  $\text{Fe}(\text{CN})_5\text{DMBP}^{3-}$ . Finally, values of  $2H_{12}$  (the splitting between potential energy curves in the intersection region)<sup>37</sup> calculated from the intervalence bands in  $\text{Ru}_2(\text{NH}_3)_{10}\text{BP}^{5+}$  and  $\text{Ru}_2(\text{NH}_3)_{10}\text{DMBP}^{5+}$  are 2.2 and 1.1 kcal/mol,<sup>23</sup> respectively.<sup>38</sup> Evidently, the coupling between Fe and Co is substantially reduced for DMBP vs BP as bridging ligands. Nevertheless, the rate constants for electron transfer are almost equal for the two complexes. It is reasonable, therefore, to infer that the two reactions are occurring in the adiabatic regime. The conclusion that the reactions are adiabatic, even when the coupling between metal centers is highly attenuated, is consistent with the theoretical estimate<sup>37</sup> of  $2H_{12} \sim 1$  kcal resulting in sufficient coupling for electron transfer to proceed in the adiabatic limit.

**Formation and Dissociation of Pentacyanoferrate(II) Complexes of Aromatic Nitrogen Heterocycles.** The rate constants for the formation and dissociation ( $k_L$  and  $k_{-L}$  in eq 3) of pentacyanoferrate(II) complexes of selected aromatic nitrogen heterocycles are listed in Table IX. Included in the table are the corresponding equilibrium constants calculated as  $k_L/k_{-L}$ . The rate constants for the formation and dissociation ( $k_f$  and  $k_d$  in Scheme I) of the binuclear complexes  $(\text{NH}_3)_5\text{CoLFe}(\text{CN})_5$  are also listed in Table IX, as are the equilibrium constants calculated as  $k_d/k_f$ . Previous studies<sup>39,40</sup> on the formation and dissociation of  $\text{Fe}(\text{CN})_5\text{L}^{3-}$

(31) Geselowitz, D. *Inorg. Chem.* **1987**, *26*, 4135.

(32) Creutz, C. *Prog. Inorg. Chem.* **1983**, *30*, 1.

(33) Some assurance that the estimates of  $\Delta G_{\text{el}}^\circ$  and  $\Delta G_{\text{in}}^\circ$  are realistic comes from a comparison between observed  $\Delta G^*$  values and those calculated from eq 9. For Pz, BP, and BPBD, observed and calculated values of  $\Delta G^*$  are 19.4 and 21.6, 21.2 and 21.2, and 22.0 and 23.0 kcal/mol, respectively.

(34) Isied, S. S.; Vassilian, A.; Wishart, J. F.; Creutz, C.; Schwarz, H. A.; Sutin, N. *J. Am. Chem. Soc.* **1988**, *110*, 635.

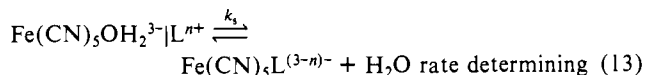
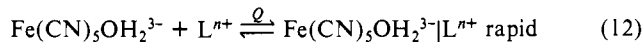
(35) Brunschwig, B. S.; Ehrenson, S.; Sutin, N. *J. Phys. Chem.* **1986**, *90*, 3657.

(36) Hush, N. S. *Coord. Chem. Rev.* **1985**, *64*, 135.

(37) Sutin, N. *Inorg. Biochem.* **1973**, *2*, 611.

(38) We have searched for the metal to metal charge-transfer bands (MMCT) of  $(\text{NH}_3)_5\text{CoBPFe}(\text{CN})_5$  and related complexes by examining their electronic spectra from the near-infrared to the ultraviolet regions but were unsuccessful. All that can be seen are the intense MLCT bands in the visible region and the strong absorption of the excess cobalt complex in the ultraviolet region. An estimate of the energy of the MMCT band for  $(\text{NH}_3)_5\text{CoBPFe}(\text{CN})_5$  can be obtained from the expression<sup>38</sup>  $E_{\text{op}} = 4\Delta G^* + E^\circ$ . With  $\Delta G^* = 21$  kcal/mol and  $E^\circ = 10$  kcal/mol, we calculate  $E_{\text{op}} = 94$  kcal/mol or 310 nm. Any MMCT band in this position would be buried under the absorption of the excess cobalt complex.

complexes have been interpreted on the basis of a dissociative or dissociative interchange mechanism. Accordingly, little variation has been found among the values of  $k_L$  for neutral ligands of different basicity.<sup>39-42</sup> On the other hand, there is a significant correlation of the rates of formation  $k_f$  with the charge type of the entering ligand.<sup>18,44,45</sup> This behavior has led to the suggestion that  $k_f$  (or  $k_L$ ) corresponds in fact to a two-step process.<sup>6,18,42</sup> In the first process contributing to  $k_f$  (or  $k_L$ ), the diffusion-controlled formation and dissociation of an encounter complex between  $\text{Fe}(\text{CN})_5\text{OH}_2^{3-}$  and the entering ligand (highly dependent on the charge of L) takes place (eq 12) and is followed by the second



step (eq 13) where rate-determining breakage of the Fe-OH<sub>2</sub> bond and coordination of the incoming ligand obtain. As expected on the basis of the two-step mechanism, values of  $k_f$  ( $=Qk_4$ ) for 3+ ligands consisting of a pentaammine moiety bound to a ligand containing an exposed, aromatic nitrogen are normally several times higher than the corresponding values measured for neutral ligands.<sup>18,19</sup> While this was found to be the case for Co-

$(\text{NH}_3)_5\text{Pz}^{3+}$ ,  $\text{Co}(\text{NH}_3)_5\text{BP}^{3+}$ , and  $\text{Co}(\text{NH}_3)_5\text{BPA}^{3+}$ , the value of  $k_f$  for  $\text{Co}(\text{NH}_3)_5\text{BPBD}^{3+}$  falls in the range of values for the neutral ligands. In fact, there is a significant trend (Table IX) in the variation of the rates of formation with the length of the bridging ligand, with longer bridges leading to smaller values of  $k_f$ . Similarly, the rate of formation of  $(\text{NC})_5\text{FePzRh}(\text{NH}_3)_5$  has been found to be about 2 times faster than for the corresponding BP complex.<sup>46</sup> The reverse trend is exhibited in the reactions of  $\text{Fe}(\text{CN})_5\text{OH}_2^{3-}$  with the negatively charged ligands  $\text{Co}(\text{CN})_5\text{L}^{2-}$ , the rate for Pz being about 6 times faster than that for BP.<sup>46</sup> An explanation of the observed trends is likely to be related to the question of dominant vs reactive ion pairs. Presumably, the dominant pairs for cationic ligands<sup>47,48</sup> correspond to the configurations  $-\text{CoNH}_3\text{NCFe}-$ , whereas the reactive ion pairs are likely to be  $-\text{CoLOH}_2\text{Fe}-$ . The equilibrium constants for the formation of the dominant ion pairs are rather insensitive to the identity of L, whereas the formation constants for the reactive ion pairs depend on the identity of L in a manner that reflects the Fe-Co distance, namely, the longer the ligand L, the smaller the formation constant of the reactive ion pair. For negatively charged ligands, the reverse trend obtains as anticipated for increasing distance between the negative charges in the reactive ion pairs.

**Acknowledgment.** This research was supported by the National Science Foundation under Grant 8502079. A.H. is indebted to Dr. Bruce Brunshwig for the calculations of the solvation energies.

**Supplementary Material Available:** Tables of observed rate constants (7 pages). Ordering information is given on any current masthead page.

- (39) Toma, H. E.; Malin, J. M. *Inorg. Chem.* **1973**, *12*, 2080.  
 (40) Bradic, Z.; Pribanic, M.; Asperger, S. *J. Chem. Soc., Dalton Trans.* **1975**, 353.  
 (41) Szecsy, A. P.; Miller, S. S.; Haim, A. *Inorg. Chim. Acta* **1978**, *28*, 189.  
 (42) Toma, H. E.; Martins, J. M.; Giesbrecht, E. *J. Chem. Soc., Dalton Trans.* **1978**, 1610.  
 (43) Hrepic, N. V.; Malin, J. M. *Inorg. Chem.* **1979**, *18*, 409.  
 (44) Malin, J. M.; Ryan, D. A.; O'Halloran, T. V. *J. Am. Chem. Soc.* **1978**, *100*, 2097.  
 (45) Katz, N. E.; Aymonino, P. J.; Blesa, M. A.; Olabe, J. A. *Inorg. Chem.* **1978**, *17*, 556.

- (46) Pfenning, K. J.; Lee, L.; Wohlers, D.; Petersen, J. D. *Inorg. Chem.* **1982**, *21*, 2477.  
 (47) Curtis, J. C.; Meyer, T. J. *Inorg. Chem.* **1982**, *21*, 1562.  
 (48) Haim, A. *Comments Inorg. Chem.* **1985**, *4*, 113.

## A New Reaction Surface for Concerted Reactions: The Metal Ion Catalyzed Addition of Enolpyruvate to Pyruvate<sup>1</sup>

Minsek Cheong and D. L. Leussing\*

Contribution from the Department of Chemistry, The Ohio State University, Columbus, Ohio 43210. Received August 22, 1988

**Abstract:** The effects of  $\text{Mg}^{2+}$  and  $\text{Zn}^{2+}$  on rates of disappearance of enzymically generated enolpyruvate along parallel ketonization and pyruvate addition paths have been measured spectrophotometrically in acetate buffers.  $\text{Zn}^{2+}$ -dependent rates of ketonization show acetate- and solvent-catalyzed pathways with rate constants of  $(3.2 \pm 0.6) \times 10^4 \text{ M}^{-2} \text{ s}^{-1}$  and  $(1.3 \pm 0.4) \times 10^2 \text{ M}^{-1} \text{ s}^{-1}$ . The former value is consistent with rate constants earlier determined<sup>4</sup> for  $\text{Mg}^{2+}$ -,  $\text{Mn}^{2+}$ -, and  $\text{Cu}^{2+}$ -dependent ketonization, and, in accordance with the Marcus function and as found with these earlier systems, the rate constant is in close agreement with the value predicted from the rate of decarboxylation of the corresponding metal ion complex of oxalacetate. Enolpyruvate adds to pyruvate in a metal ion dependent step to yield pyruvate dimer (I), according to the rate law  $\text{rate}_{\text{dimer formation}} = k[\text{M}^{2+}][\text{HEP}][\text{PYRU}]$  with  $k = (1.2 \pm 0.1) \times 10^4 \text{ M}^{-2} \text{ s}^{-1}$  ( $\text{Zn}^{2+}$ ) and  $(4.3 \pm 0.6) \times 10^2 \text{ M}^{-2} \text{ s}^{-1}$  ( $\text{Mg}^{2+}$ ). Reaction surfaces obtained by averaging Albery and modified Guthrie surfaces were found to provide calculated rate constants that are in good agreement with the observed values using an intrinsic barrier for carbon-carbon bond formation obtained from OH<sup>-</sup>-dependent rates reported for aldol condensation and the retroaldol condensation of 3-penten-2-one. In the reaction model it is assumed that carbon-carbon bond formation is concerted with proton transfer and occurs within the coordination sphere of a metal ion-mixed ligand complex. The calculations indicate that in the transition state carbon-carbon bond formation leads proton transfer and occurs to the same extent with both metal ions. The metal ions aid in stabilizing the negative charge that appears on the pyruvate keto oxygen atom as carbon-carbon bond formation proceeds. Proton transfer from the enol oxygen atom also aids in this process, with a greater portion of the stabilization being assumed by the proton in the case of the more weakly binding  $\text{Mg}^{2+}$  ion.

How metal ions influence the reactivities of ligands that are bound to them has intrigued chemists for many years. In general,

studies in this area have tended to focus on one of two broad categories of metal ions: inert and labile. In either case ambi-